

Combinatorial-Topological Framework for the Analysis of Global Dynamics

Justin Bush* Marcio Gameiro[†] Shaun Harker[‡]
Hiroshi Kokubu[§] Konstantin Mischaikow[¶]
Ippei Obayashi^{||} Paweł Pilarczyk^{**}

April 26, 2012

Abstract

We discuss an algorithmic framework based on efficient graph algorithms and algebraic-topological computational tools. The framework is aimed at automatic computation of a database of global dynamics of a given m -parameter semidynamical system with discrete time on a bounded subset of the n -dimensional phase space. We introduce the

*Department of Mathematics, Hill Center-Busch Campus, Rutgers, The State University of New Jersey, 110 Frelinghusen Rd, Piscataway, NJ 08854-8019, USA (e-mail address: bushjc@math.rutgers.edu).

[†]Instituto de Ciências Matemáticas e de Computação, Universidade de São Paulo, Caixa Postal 668, 13560-970, São Carlos, SP, Brazil (e-mail address: gameiro@icmc.usp.br).

[‡]Department of Mathematics, Hill Center-Busch Campus, Rutgers, The State University of New Jersey, 110 Frelinghusen Rd, Piscataway, NJ 08854-8019, USA (e-mail address: sharker@math.rutgers.edu).

[§]Department of Mathematics / JST CREST, Kyoto University, Kyoto 606-8502, Japan (e-mail address: kokubu@math.kyoto-u.ac.jp).

[¶]Department of Mathematics and BioMaPS, Hill Center-Busch Campus, Rutgers, The State University of New Jersey, 110 Frelinghusen Rd, Piscataway, NJ 08854-8019, USA (e-mail address: mischaik@math.rutgers.edu).

^{||}Department of Mathematics / JST CREST, Kyoto University, Kyoto 606-8502, Japan (e-mail address: obayashi@math.kyoto-u.ac.jp).

^{**}Centre of Mathematics, University of Minho, Campus de Gualtar, 4710-057 Braga, Portugal (e-mail address: pawel.pilarczyk@math.uminho.pt).

mathematical background, which is based upon Conley's topological approach to dynamics, describe the algorithms for the analysis of the dynamics using rectangular grids both in phase space and parameter space, and show two sample applications.

Key words and phrases: dynamical system, Morse decomposition, Conley index, grid decomposition, graph algorithms, rigorous numerics

It is well established that multiparameter nonlinear dynamical systems exhibit extremely complex behavior. For many applications, especially multiscale problems or in settings in which precise measurements are difficult, an understanding of coarse but robust structures that exist over large ranges of parameter values is of greater importance than a detailed understanding of the fine structure. With this in mind we discuss a new mathematical and computational framework for the analysis of the global dynamics of multiparameter nonlinear systems. Our approach is based on a finite combinatorial approximation of phase space, parameter space and the nonlinear dynamics. This is used to obtain a description of the global dynamics in terms of acyclic directed graphs called Morse graphs. A rigorous understanding of the dynamics is obtained using the Conley index, an algebraic topological invariant. The resulting information is finite and presented in the form of graphs and algebraic invariants and thus can be easily queried. For this reason we view our procedure as producing a database for the global nonlinear dynamics for a parameterized nonlinear system. We include a discussion concerning the computational complexity of our approach along with two simple illustrative examples.

1 Introduction

Physical models of evolutionary processes are typically framed in terms of continuous state spaces, parameter spaces and time. Understanding the existence, structure and bifurcation of invariant sets often forms the focal point for the qualitative study of these systems. However, the theoretical work of the last century makes clear that invariant sets can possess structure on all spatial and temporal scales and furthermore that these structures can vary dramatically over parameter sets which can be as complicated as Cantor sets of positive measure.

These results need to be contrasted with available methods of analysis, the ability to make measurements, and the derivation of models. In the

context of applications the focus is often on understanding the dynamics of a particular parameterized family of nonlinear systems. Because of the nonlinearity, typically this analysis is heavily dependent on performing and interpreting numerical simulations. Furthermore, these results are often compared against experimental data which itself is limited to finite measurements that contain errors and are of limited precision. Finally, many mathematical models, especially those arising from multiscale systems, are heuristic in nature; that is, the nonlinearities are not derived from first principle, but rather through a series of approximations. This implies that the exact values produced by the model at particular parameter values cannot be expected to and are not intended to exactly match those of the physical system. In addition, there are many instances of models for which crucial parameter values are unknown with bounds that range over many orders of magnitude.

This gap between the potentially infinite complexity of invariant sets and the crude tools of analysis and measurement suggests that an alternative perspective in describing the global properties of multiparameter families of nonlinear dynamical systems may be of use. In this paper we provide a review of our attempts to develop such a new perspective with a focus on the computational aspects of the approach.

To keep technicalities to a minimum, we consider a multiparameter dynamical system given in the form of a continuous map

$$\begin{aligned} f: \mathbb{R}^n \times \mathbb{R}^m &\rightarrow \mathbb{R}^n \\ (x, z) &\mapsto f_z(x) := f(x, z) \end{aligned} \tag{1}$$

where \mathbb{R}^n is the phase space and \mathbb{R}^m is the parameter space. However, it should be noted that this is not a serious restriction. Techniques that are analogous to those described in this paper have been successfully employed to study the dynamics of ordinary differential equations,^[18] partial differential equations,^[5] infinite dimensional maps,^[4] fast-slow systems^[7] and time series analysis.^[16] Let $X \subset \mathbb{R}^n$ be a compact subset of phase space that contains the dynamics of interest and let $Z \subset \mathbb{R}^m$ be a compact subset of parameter space which contains the set of physically relevant parameters. Our goal is to provide a mathematically rigorous description of the global dynamics restricted to X for all parameter values in Z .

Recall that for a given parameter value $z \in Z$, $S_z \subset X$ is an *invariant set* under f_z if $f_z(S_z) = S_z$. Traditionally, invariant sets are the focal point for dynamical systems. In the approach we present here, they play a secondary

role. Instead, we focus on *isolating neighborhoods*; these are compact sets $N \subset X$ such that

$$\text{Inv}(N, f_z) \subset \text{int}(N)$$

where $\text{Inv}(N, f_z)$ denotes the maximal invariant set contained in N and $\text{int}(N)$ denotes the interior of N . Simple arguments based on continuity show that if N is an isolating neighborhood for f_z , then it is an isolating neighborhood for $f_{z'}$ for all z' sufficiently close to z . An invariant set that is the maximal invariant set in an isolating neighborhood is called an *isolated invariant set*. Given an isolating neighborhood, information about the isolated invariant set can be extracted using the Conley index which is discussed in greater detail in Sections 2.3 and 2.4. For the moment it is sufficient to make three remarks.

- N1** One can associate a Conley index to any isolating neighborhood.
- N2** If N and N' are isolating neighborhoods and $\text{Inv}(N, f_z) = \text{Inv}(N', f_z)$, then they have the same Conley index.
- N3** If N is an isolating neighborhood for all z in a path connected subset of Z , then the Conley index associated with N is the same for all f_z .

For justification of these remarks and further information about the Conley index see Ref. [17]. The theme of this work is that isolating neighborhoods are relatively easy to identify, their Conley indices can be computed, and thus we can obtain information about isolated invariant sets. **N2** suggests that this information is relatively insensitive to the numerical approximations used to identify the isolating neighborhood. Furthermore, **N3** implies that the dynamical information extracted using the Conley index is robust with respect to perturbations in parameter values.

2 Mathematical Framework

Because we are interested in structures which are invariant with respect to perturbations in parameter space, it is convenient to consider the parameterized dynamical system

$$\begin{aligned} F: \mathbb{R}^n \times \mathbb{R}^m &\rightarrow \mathbb{R}^n \times \mathbb{R}^m \\ (x, z) &\mapsto (f_z(x), z) \end{aligned} \tag{2}$$

Given $Z \subset \mathbb{R}^m$, we denote the restriction of F to $\mathbb{R}^m \times Z$ by $F_Z: \mathbb{R}^n \times Z \rightarrow \mathbb{R}^n \times Z$.

2.1 Approximating Dynamics

We can only perform a finite number of calculations, thus we need to combinatorialize phase space, parameter space, and the map that generates the dynamics. The discretization of phase space and parameter space is done using the concept of a *grid*.^[20] This consists of a finite collection \mathcal{X} of nonempty, compact subsets of X with the following properties:

- (a) $X = \bigcup_{\xi \in \mathcal{X}} \xi$;
- (b) $\xi = \text{cl}(\text{int}(\xi))$ for all $\xi \in \mathcal{X}$;
- (c) $\xi \cap \text{int}(\xi') = \emptyset$ for all $\xi \neq \xi'$.

The *diameter* of a grid \mathcal{X} is defined by

$$\text{diam}(\mathcal{X}) = \sup_{\xi \in \mathcal{X}} \text{diam}(\xi).$$

As shown in Ref. [12], any compact metric space admits a grid of arbitrarily small diameter. For $\mathcal{A} \subset \mathcal{X}$, the set $\bigcup_{\xi \in \mathcal{A}} \xi \subset X$ is denoted by $|\mathcal{A}|$.

For the sake of simplicity, in this paper we will only consider grids with grid elements in the form of cubes or simplices. With this in mind, we restrict the regions of phase space $X \subset \mathbb{R}^n$ and parameter space $Z \subset \mathbb{R}^m$ to be sets that can be represented by cubical or simplicial grids \mathcal{X} and \mathcal{Z} , respectively.

To discretize the dynamics, we make use of a *combinatorial multivalued map* $\mathcal{F}: \mathcal{X} \rightrightarrows \mathcal{X}$ which assigns to each element of a grid $\xi \in \mathcal{X}$ a subset (possibly empty) $\mathcal{F}(\xi)$ of \mathcal{X} . With regard to the algorithms that are employed in the analysis of the dynamics, it is important to observe that a combinatorial multivalued map is equivalent to a finite directed graph with vertices \mathcal{X} and directed edges (ξ, ξ') whenever $\xi' \in \mathcal{F}(\xi)$. With this in mind, we will refer to \mathcal{F} as a multivalued map or a directed graph, whichever is more convenient or intuitive given the situation.

To understand the relationship between multivalued maps and nonlinear dynamics, consider a continuous function $f: \mathbb{R}^n \rightarrow \mathbb{R}^n$ and a compact subset $X \subset \mathbb{R}^n$. Let \mathcal{X} be a grid for X . A combinatorial multivalued map $\mathcal{F}: \mathcal{X} \rightrightarrows \mathcal{X}$ is an *outer approximation* of f , if

$$f(\xi) \subset \text{int}(|\mathcal{F}(\xi)|) \quad \text{for all } \xi \in \mathcal{X}. \quad (3)$$

Given a grid \mathcal{X} , the minimal outer approximation of f is given by

$$\tilde{\mathcal{F}}(\xi) := \{\xi' \mid \xi' \cap f(\xi) \neq \emptyset\}$$

and any other outer approximation \mathcal{F} of f satisfies $\tilde{\mathcal{F}}(\xi) \subset \mathcal{F}(\xi)$ for all $\xi \in \mathcal{X}$.^[12]

An important observation is the fact that if $\tilde{\mathcal{F}}$ is a minimal outer approximation of f , then there exists $\delta > 0$ such that if $\|g(x) - f(x)\| < \delta$ for all $x \in X$ then $\tilde{\mathcal{F}}$ is an outer approximation of g . Another outer approximation \mathcal{F} for f , which is not minimal, will in general allow for a larger δ . In this sense, grids and outer approximations provide a robust approximation of dynamics.

From the computational perspective, determining the minimal outer approximation is typically too expensive. In general, the best that can be done is to compute an approximation of $f(\xi)$ along with an error bound ε which may or may not be small. With this information one can construct an outer approximation that satisfies the following condition

$$\{\xi' \in \mathcal{X} \mid \xi' \cap B_\varepsilon(f(\xi)) \neq \emptyset\} \subset \mathcal{F}(\xi).$$

The focus of this paper is on parameterized dynamical systems (2) for which we have chosen grids \mathcal{X} and \mathcal{Z} for X and Z , the regions of interest in phase space and parameter space, respectively. For each $\zeta \in \mathcal{Z}$, let $\mathcal{F}_\zeta: \mathcal{X} \rightrightarrows \mathcal{X}$ be an outer approximation of $F_\zeta: \mathbb{R}^n \times \zeta \rightarrow \mathbb{R}^n \times \zeta$ restricted to the grid $\mathcal{X} \times \zeta := \{\xi \times \zeta \mid \xi \in \mathcal{X}\}$. By definition, this implies that

$$f(\xi, \zeta) \subset \text{int}(|\mathcal{F}_\zeta(\xi)|) \quad \text{for all } \xi \in \mathcal{X}$$

To understand how \mathcal{F}_ζ acts as an approximation of the underlying dynamics induced by (1), we state the following proposition which follows directly from the definition of an outer approximation.

Proposition 2.1. *Let \mathcal{F}_ζ be an outer approximation for F_ζ . Consider any $x \in \xi$ and any ordered sequence of parameter values (z_1, z_2, \dots, z_T) where $\{z_i \in \zeta \mid i = 1, \dots, T\}$. Define*

$$x_{i+1} := f_{z_i}(x_i)$$

where $x_0 = x$ and choose $\xi_i \in \mathcal{X}$ such that $x_i \in \xi_i$. Then the ordered sequence $(\xi, \xi_1, \dots, \xi_{T+1})$ is a path in the directed graph \mathcal{F}_ζ .

2.2 Extracting Nonrecurrent Dynamics

Assume that the grids \mathcal{X} , \mathcal{Z} are chosen and for a fixed $\zeta \in \mathcal{Z}$ an outer approximation $\mathcal{F}_\zeta: \mathcal{X} \rightrightarrows \mathcal{X}$ has been computed. The first step in using our approximation scheme to understand the dynamics generated by (1) is to identify the nonrecurrent dynamics.

Given the directed graph \mathcal{F}_ζ and $\mathcal{N} \subset \mathcal{X}$, the associated *subgraph* is the directed graph $\mathcal{F}_\zeta|_{\mathcal{N}}: \mathcal{N} \rightrightarrows \mathcal{N}$ consisting of the vertices $\{\xi \in \mathcal{N}\}$ and edges $\{(\xi, \xi') \mid \xi, \xi' \in \mathcal{N}, \xi' \in \mathcal{F}_\zeta(\xi)\}$. A directed graph is *invariant* if each vertex is both the head of at least one edge and the tail of at least one edge.

Proposition 2.2. *Let $\mathcal{S}_\zeta \subset \mathcal{X}$ be the maximal invariant subgraph of \mathcal{F}_ζ . Then*

$$\text{Inv}(X, f_z) \subset |\mathcal{S}_\zeta|$$

for all $z \in \zeta$.

The proof follows directly from Proposition 2.1. A consequence of Proposition 2.2 is that we have identified the portion of phase space on which the asymptotic dynamics takes place for all parameter values $z \in \zeta$. The next step is to identify the relevant dynamical structures which, likewise, are invariant for all $z \in \zeta$.

Given the directed graph \mathcal{F}_ζ , two elements $\xi, \xi' \in \mathcal{X}$ belong to the same *strongly connected path component* if there exist nontrivial paths from ξ to ξ' and ξ' to ξ .

Definition 2.3. Given a directed graph \mathcal{F}_ζ , the collection of all strongly connected path components

$$\{\mathcal{M}_\zeta(p) \subset \mathcal{X} \mid p \in \mathbb{P}_\zeta\}$$

is the *Morse decomposition* of \mathcal{F}_ζ . The individual strongly connected path components are called *Morse sets*.

The proof of the following proposition follows from direct applications of the definition of strongly connected path components, the definition of \mathcal{S}_ζ and Proposition 2.1.

Proposition 2.4. *Consider an outer approximation $\mathcal{F}_\zeta: \mathcal{X} \rightrightarrows \mathcal{X}$ of F_ζ with maximal invariant subgraph generated by \mathcal{S}_ζ . Then:*

1. $\mathcal{M}_\zeta(p) \subset \mathcal{S}_\zeta$ for all $p \in \mathbb{P}_\zeta$.

2. If $p \neq q$, then $\mathcal{M}_\zeta(p) \cap \mathcal{M}_\zeta(q) = \emptyset$
3. If $\xi \in \mathcal{S}_\zeta \setminus \bigcup_{p \in \mathcal{P}_\zeta} \mathcal{M}_\zeta(p)$, then there exists $p, q \in \mathcal{P}_\zeta$ and a path in \mathcal{F}_ζ that begins in $\mathcal{M}(p)$, passes through ξ , and ends in $\mathcal{M}(q)$. Note: If such a path exists for some $p, q \in \mathcal{P}_\zeta$ then we write $q <_\zeta p$.
4. If $x \in \xi$ and $\xi \in \mathcal{S}_\zeta \setminus \bigcup_{p \in \mathcal{P}_\zeta} \mathcal{M}_\zeta(p)$, then x is not a recurrent point of f_z restricted to X for all $z \in \zeta$.
5. Under the relationship \leq_ζ , defined above, \mathcal{P}_ζ is a partially ordered set.

Proposition 2.5 (See Theorem 4.1 in Ref. [12]). *Let $\{\mathcal{M}_\zeta(p) \subset \mathcal{X} \mid p \in \mathcal{P}_\zeta\}$ be the Morse decomposition for the outer approximation $\mathcal{F}_\zeta: \mathcal{X} \rightrightarrows \mathcal{X}$ of F_ζ . Then for all $p \in \mathcal{P}_\zeta$, $|\mathcal{M}_\zeta(p)|$ is an isolating neighborhood for f_z for all $z \in \zeta$.*

Recall that given a partially ordered set (\mathcal{P}, \leq) , we say that q covers p if from the relation $q \leq r \leq p$ it follows that either $q = r$ or $r = p$.

Definition 2.6. The Morse graph MG_ζ of \mathcal{F}_ζ is the acyclic directed graph with nodes consisting of the Morse sets and directed edges $\mathcal{M}_\zeta(p) \rightarrow \mathcal{M}_\zeta(q)$ if and only if q covers p in (\mathcal{P}, \leq) .

2.3 Identifying Recurrent Dynamics

For each grid element ζ in parameter space, the associated Morse graph MG_ζ provides rigorous information about the nonrecurrent dynamics and potential information about the recurrent dynamics that is valid over all parameter values in $|\zeta| \subset Z$. In particular, if recurrent dynamics occurs for some parameter value then it must occur within a region determined by a Morse set. We now describe the Conley index, which is an algebraic topological tool that can provide information about the recurrent dynamics.

We begin our description by considering an arbitrary continuous map $g: Y \rightarrow Y$ defined on a locally compact metric space. Consider a pair of compact sets $P = (P_1, P_0)$ with $P_0 \subset P_1$. Let $(P_1/P_0, [P_0])$ denote the pointed topological space where P_1/P_0 is the quotient space obtained by collapsing P_0 to a single point denoted by $[P_0]$. Let $g_P: (P_1/P_0, [P_0]) \rightarrow (P_1/P_0, [P_0])$ be defined by

$$g_P([x]) = \begin{cases} f(x) & \text{if } x, f(x) \in P_1 \setminus P_0; \\ [P_0] & \text{otherwise} \end{cases}$$

Definition 2.7. A pair of compact sets $P = (P_1, P_0)$ is an *index pair* for g if

1. g_P is continuous, and
2. $\text{cl}(P_1 \setminus P_0)$ is an isolating neighborhood under g .

The induced map g_P is called an *index map*.

Because we have assumed that our grids are defined in terms of cubes or simplices, we obtain the following result which implies that we can find index pairs associated with each of the regions that contain the potentially recurrent dynamics.

Proposition 2.8. *Let $\{\mathcal{M}_\zeta(p) \subset \mathcal{X} \mid p \in \mathbf{P}_\zeta\}$ be the Morse decomposition for the outer approximation $\mathcal{F}_\zeta: \mathcal{X} \rightrightarrows \mathcal{X}$ of F_ζ . Assume $|\mathcal{S}_\zeta| \subset \text{int}(X)$. Let $P = (P_1, P_0)$ be defined by*

$$P_1 := |\mathcal{F}_\zeta(\mathcal{M}_\zeta(p))| \quad \text{and} \quad P_0 := |\mathcal{F}_\zeta(\mathcal{M}_\zeta(p)) \setminus \mathcal{M}_\zeta(p)|$$

Then for all $z \in \zeta$, P is an index pair for f_z .

Given an index pair P for g , the continuity of g_P implies that the following family of induced maps on homology is well defined

$$g_{P,k}: H_k(P_1/P_0, [P_0]) \rightarrow H_k(P_1/P_0, [P_0]), \quad k = 0, 1, 2, \dots$$

This is a representative of the Conley index (which is defined later) for the isolating neighborhood $\text{cl}(P_1 \setminus P_0)$ under g . Computations can be done using rational coefficients in which case

$$g_{P,k}: H_k(P_1/P_0, [P_0], \mathbb{Q}) \rightarrow H_k(P_1/P_0, [P_0], \mathbb{Q}), \quad k = 0, 1, 2, \dots$$

is a linear map on a vector space, and the nonzero eigenvalues $\bar{\sigma}_k$ of $g_{P,k}$ can be used as a representative of the Conley index.

The most fundamental result associated with the Conley index is the following

Theorem 2.9 (See Ref. [17]). *Let $g_{P,k}: H_k(P_1/P_0, [P_0]) \rightarrow H_k(P_1/P_0, [P_0])$ be induced by index maps. If for some $k \in 0, 1, 2, \dots$, $g_{P,k}$ is not nilpotent, then*

$$\text{Inv}(\text{cl}(P_1 \setminus P_0), g) \neq \emptyset.$$

The following theorem provides a simple example of how the Conley index can be used to extract more detailed information about the dynamics that is robust with respect to perturbations in parameter space

Theorem 2.10. *Let $\mathcal{M}_\zeta(p)$ be a Morse set for the outer approximation $\mathcal{F}_\zeta: \mathcal{X} \rightrightarrows \mathcal{X}$ of F_ζ . Then*

$$\bar{\sigma}_0 = \emptyset \quad \text{or} \quad \bar{\sigma}_0 = \left\{ e^{2\pi i \frac{k}{T}} \mid k = 0, \dots, T-1 \right\} \text{ for some } T > 0.$$

In the latter case,

$$|\mathcal{M}_\zeta(p)| = \bigcup_{i=0}^{T-1} N_i$$

where $\{N_i \mid i = 0, \dots, T-1\}$ are mutually disjoint compact sets with the property that

$$F_\zeta(N_i) \subset N_{i+1}, \quad i = 0, \dots, T-1$$

and

$$F_\zeta(N_{T-1}) \subset N_0.$$

In particular, given any sequence of parameter values $\{z_j \mid j = 0, 1, 2, \dots\} \subset \zeta$, any $x_0 \in N_0$ and $x_{j+1} := f_{z_j}(x_j)$, we have

$$x_{j+1} \in N_k \quad \text{where } k = j+1 \pmod T.$$

The proof of this theorem follows from Ref. [2, Proposition 5.8] and Proposition 2.1.

Definition 2.11. The *Conley-Morse graph* CMG_ζ of \mathcal{F}_ζ consists of the Morse graph MG_ζ of \mathcal{F}_ζ along with the Conley index associated with each Morse set $\mathcal{M}_\zeta(p)$, $p \in \mathbb{P}_\zeta$.

It is important to note that given an index pair as in Proposition 2.8, the induced map on homology of an associated index map can be computed using \mathcal{F}_ζ .^[11, 19, 9]

2.4 Classifying Dynamics over Parameter Space

The discussion in Sections 2.1 and 2.3 is restricted to the dynamics of F_ζ where $\zeta \in \mathcal{Z}$ is a single grid element in parameter space. Since the results are valid for every $\zeta \in \mathcal{Z}$, this provides a rigorous description of the dynamics

for every point $z \in Z$. What remains to be discussed is how the dynamics over different grid points $\zeta, \zeta' \in \mathcal{Z}$ are related. We begin by defining a relationship between the Morse sets.

Definition 2.12. Let $\zeta, \zeta' \in \mathcal{Z}$ such that $\zeta \cap \zeta' \neq \emptyset$. The *clutching graph* $\mathcal{I}(\zeta, \zeta')$ is the bipartite graph with vertices $\mathbf{P}_\zeta \cup \mathbf{P}_{\zeta'}$ and with edges

$$(p, q) \in \mathbf{P}_\zeta \times \mathbf{P}_{\zeta'} \quad \text{if and only if} \quad \mathcal{M}_\zeta(p) \cap \mathcal{M}_{\zeta'}(q) \neq \emptyset.$$

Proposition 2.13. *Assume there is a unique edge (p, q) in the clutching graph $\mathcal{I}(\zeta, \zeta')$ that has either p or q as its endpoint. Then the Conley index of $|\mathcal{M}_\zeta(p)|$ under F_ζ is the same as the Conley index of $|\mathcal{M}_{\zeta'}(q)|$ under $F_{\zeta'}$.*

Proof. Let $z \in \zeta \cap \zeta'$. By Proposition 2.5, $|\mathcal{M}_\zeta(p)|$ and $|\mathcal{M}_{\zeta'}(q)|$ are isolating neighborhoods. Let $S_z := \text{Inv}(|\mathcal{M}_\zeta(p)|, f_z)$ and $S'_z := \text{Inv}(|\mathcal{M}_{\zeta'}(q)|, f_z)$. Observe that it is sufficient to show that $S_z = S'_z$, since the result then follows from **N2**.

With this in mind, suppose $S_z \neq S'_z$. Without loss of generality we can assume that there exists $x \in S_z \setminus S'_z$. This implies that there is a grid element $\xi \in \mathcal{X}$ such that $x \in \xi \in \mathcal{M}_\zeta(p) \setminus \mathcal{M}_{\zeta'}(q)$. Since $x \in S_z$, ξ belongs to a strongly connected path component and hence belongs to $\mathcal{M}_{\zeta'}(r)$ for some $r \in \mathbf{P}_{\zeta'}$ where $r \neq q$. This implies that the clutching graph $\mathcal{I}(\zeta, \zeta')$ contains the edge (p, r) , contradicting the uniqueness of the edges with endpoint p . \square

The key step in the proof of Proposition 2.13 is **N2**. Observe that the validity of **N2** is not obvious. In general, the index pairs $P = (P_1, P_0)$ defined by

$$P_1 := |\mathcal{F}_\zeta(\mathcal{M}_\zeta(p))| \quad \text{and} \quad P_0 := |\mathcal{F}_\zeta(\mathcal{M}_\zeta(p)) \setminus \mathcal{M}_\zeta(p)|$$

and $P' = (P'_1, P'_0)$ defined by

$$P'_1 := |\mathcal{F}_{\zeta'}(\mathcal{M}_{\zeta'}(q))| \quad \text{and} \quad P'_0 := |\mathcal{F}_{\zeta'}(\mathcal{M}_{\zeta'}(q)) \setminus \mathcal{M}_{\zeta'}(q)|$$

will be different and hence the induced index maps

$$f_{P,k}: H_k(P_1/P_0, [P_0]) \rightarrow H_k(P_1/P_0, [P_0])$$

and

$$f_{P',k}: H_k(P'_1/P'_0, [P'_0]) \rightarrow H_k(P'_1/P'_0, [P'_0])$$

will provide different representations of the Conley index. Thus to explain **N2** requires a discussion of the equivalence classes used to define the Conley index. This is best done in a fairly general setting, so consider two functions

$$a: V \rightarrow V \quad \text{and} \quad b: W \rightarrow W$$

where V and W are both either finitely generated abelian groups or finite dimensional vector spaces, and a and b are group homomorphisms or linear maps.

Definition 2.14. The maps a and b are *shift equivalent* if there exist morphisms

$$r: V \rightarrow W \quad \text{and} \quad s: W \rightarrow V$$

such that

$$b \circ r = r \circ a \quad \text{and} \quad s \circ b = a \circ s$$

and a positive integer n such that

$$s \circ r = a^n \quad \text{and} \quad r \circ s = b^n.$$

From Ref. [6] it follows that if $f_{P,k}$ and $f_{P',k}$ are constructed as above, then $f_{P,k}$ and $f_{P',k}$ are shift equivalent. More generally, when we indicate that two Conley indices agree then we mean that the representative index maps are shift equivalent.

Proposition 2.13 motivates the following definition.

Definition 2.15. Fix grids \mathcal{X} and \mathcal{Z} and outer approximations $\mathcal{F}_\zeta: \mathcal{X} \rightrightarrows \mathcal{X}$ for all $\zeta \in \mathcal{Z}$. Two Morse sets $M_\zeta(p)$ and $M_{\zeta'}(p')$ belong to the same *Morse continuation class* if there exists a sequence of grid elements $\{\zeta_i \mid i = 0, \dots, I\}$ with $\zeta_0 = \zeta$, $\zeta_I = \zeta'$ and indexing elements $\{p_i \in \mathbf{P}_{\zeta_i} \mid i = 0, \dots, I\}$ with $p_0 = p$, $p_I = p'$ such that for all $i = 0, \dots, I - 1$ there exists a unique edge (p_i, p_{i+1}) in the clutching graph $\mathcal{I}(\zeta_i, \zeta_{i+1})$ that has either p_i or p_{i+1} as its endpoint.

N3 combined with Proposition 2.13 leads to the following result.

Corollary 2.16. *Let $M_\zeta(p)$ and $M_{\zeta'}(p')$ belong to the same continuation class. Let $z \in \zeta$ and $z' \in \zeta'$. Then the Conley index of $|\mathcal{M}_\zeta(p)|$ under f_z is the same as the Conley index of $|\mathcal{M}_{\zeta'}(p')|$ under $f_{z'}$.*

Remark 2.17. It is possible that $\mathcal{M}_\zeta(p)$ and $\mathcal{M}_\zeta(q)$, $q, p \in \mathbf{P}_\zeta$, belong to the same continuation class even if $p \neq q$.

Extending the idea of continuation classes to Morse graphs is slightly more subtle. Assume that the clutching graph $\mathcal{I}(\zeta, \zeta')$ has the property that each node is the endpoint of exactly one edge. This defines a bijection

$$\begin{aligned} b_{\zeta, \zeta'}: \mathbf{P}_\zeta &\rightarrow \mathbf{P}_{\zeta'} \\ p &\mapsto q \end{aligned} \tag{4}$$

if (p, q) is an edge of $\mathcal{I}(\zeta, \zeta')$.

Definition 2.18. Fix grids \mathcal{X} and \mathcal{Z} and outer approximations $\mathcal{F}_\zeta: \mathcal{X} \rightrightarrows \mathcal{X}$ for all $\zeta \in \mathcal{Z}$. Two Conley-Morse graphs CMG_ζ and $\text{CMG}_{\zeta'}$ belong to the same *Conley-Morse graph continuation class* if there exists a sequence of grid elements $\{\zeta_i \mid i = 0, \dots, I\}$ with $\zeta_0 = \zeta$, $\zeta_I = \zeta'$ and indexing elements $\{p_i \in \mathbf{P}_{\zeta_i} \mid i = 0, \dots, I\}$ with $p_0 = p$, $p_I = p'$ such that for all $i = 0, \dots, I-1$ the bijection

$$b_{\zeta_i, \zeta_{i+1}}: (\mathbf{P}_{\zeta_i}, \leq_{\zeta_i}) \rightarrow (\mathbf{P}_{\zeta_{i+1}}, \leq_{\zeta_{i+1}})$$

is a directed graph isomorphism

Remark 2.19. To each Conley-Morse graph continuation class, we associate three distinct types of information:

- The Morse graph, which provides information about the structure of the non-recurrent dynamics.
- The Conley indices of the Morse sets, which provide information about the structure of the recurrent dynamics.
- The set of parameter grid elements whose Conley-Morse graphs belong to the Conley-Morse continuation class. This provides a lower bound on the set of parameter values at which the identified recurrent and non-recurrent dynamics must occur. We use the number of parameter grid elements to measure the *size* of the continuation class.

Remark 2.20. The information about the dynamics provided by our approach can be viewed as a database of dynamics for the multiparameter nonlinear dynamical system (1) restricted to the region of phase space $X \subset \mathbb{R}^n$ and parameter space $Z \subset \mathbb{R}^m$ where the minimal levels of resolution are

determined by the diameters of the grids \mathcal{X} and \mathcal{Z} . In particular, we can construct the *continuation graph*; that is, a graph whose nodes consist of the Conley-Morse graph continuation classes and whose edges consist of the clutching graph information between representative Conley-Morse graphs. This type of information is exhibited in Figure 2.4 for the overcompensatory Leslie model^[22]

$$\begin{bmatrix} x \\ y \end{bmatrix} \mapsto \begin{bmatrix} x(\theta_1 x + \theta_2 y)e^{-0.1(x+y)} \\ 0.7x \end{bmatrix} \quad (5)$$

To limit the information to a comprehensible amount, the upper left corner indicates the continuation graph associated with the 26 largest Conley-Morse graph continuation classes.

2.5 Grid Refinements and Bifurcations

The accuracy of computations is affected by a variety of factors, including the method for construction of combinatorial multivalued maps, but the size of the grid in phase space and parameter space is the most prominent factor that may affect the structure of the constructed Conley-Morse graphs. In general, at finer grids some Morse sets may be split and the finer structure of dynamics in their regions may be revealed. As a consequence, the complexity of the Conley-Morse graphs depends on the grid size. Namely, if the parameter value is fixed, the Conley-Morse graph on a finer grid may be larger than that on a coarser grid, as long as Morse sets with non-trivial Conley index are concerned. To be more precise, recall that the Conley-Morse graph and its subgraph consisting of Morse sets with non-trivial Conley index are posets (partially-ordered sets). The poset of the subgraph on a finer grid is projected *onto* the poset on a coarser grid by a map naturally induced by the grid refinement.

The same relation holds true for parameter grid refinement. Namely, for a parameter grid element and one of its refined parameter grid elements, the corresponding poset of the subgraph on a finer parameter grid element is projected *onto* the poset on a coarser parameter grid element by a map naturally induced by the parameter inclusion.

One of the problems that must be dealt with in the construction of Conley-Morse graphs is the appearance of Morse sets with trivial Conley index. Because of the trivial index, one cannot prove that their invariant part is nonempty, and in fact, for some systems, hundreds or thousands of

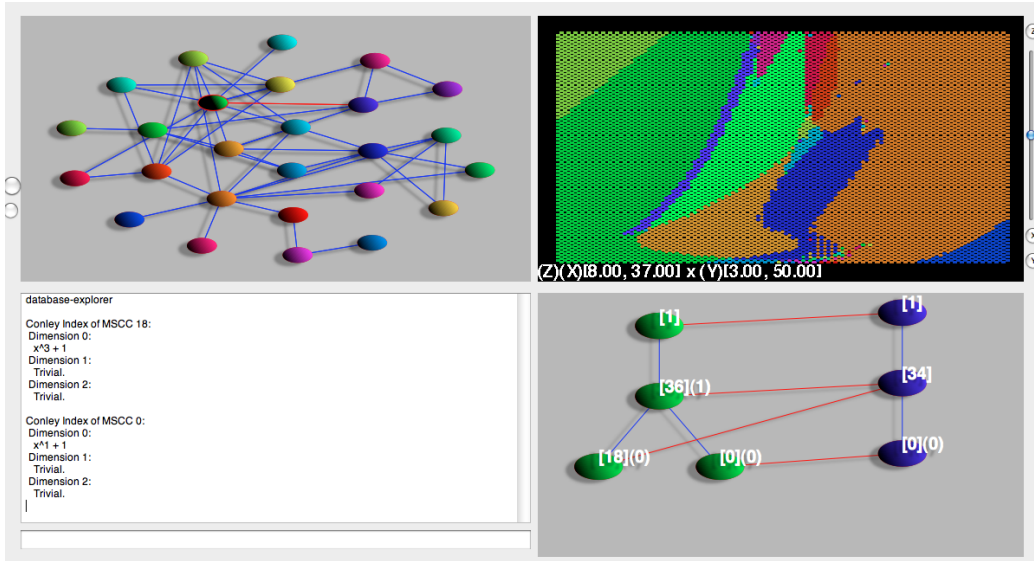


Figure 1: Database information concerning dynamics for the overcompensatory Leslie model (5). (Upper Left) Continuation Graph: Each node corresponds to a Conley-Morse graph equivalence class. Each edge corresponds to a clutching graph between Conley-Morse graphs. (Upper Right) Parameter space divided into regions corresponding to Conley-Morse graph equivalence classes. Color coding of parameter space matches the color coding of the nodes in the continuation graph. (Lower Right) Clutching graph between two Conley-Morse graphs. This clutching graph corresponds to the highlighted (red) edge in the continuation graph. The nodes of the Conley-Morse graphs have two types of labels $[*]$ and $(*)$. The square brackets indicate the Morse continuation class associated with the node. The parenthesis indicate the level of homology on which the Conley index is non trivial. (Lower Left) Conley indices of the Morse sets. The polynomial is the invariant factor for the shift equivalence class of the linear map on homology using \mathbb{Z}_2 coefficients induced by the index map.

such “spurious” sets isolating the empty set may appear. A powerful method for detecting such Morse sets in order to prune them and reduce the Morse graphs is to refine the grid in such a set and check for the emptiness of its invariant part at the higher resolution.^[2] Therefore, if a Morse set does not appear to have the empty invariant part after several refinements then this is an indication of the presence of non-trivial dynamics and a possibility of bifurcation. See Ref. [1] for an analysis of the saddle-node bifurcation from this point of view.

3 Algorithms

The mathematical framework proposed in Section 2 is combinatorial in nature and the presented motivation was the need for a robust description of dynamics with respect to both parameters and measurement. In this section we change the perspective and observe that a combinatorial theory raises hopes that the dynamical structures being extracted are computable. Of course, the practicality of these computations depends upon the availability, development and implementation of efficient algorithms.

3.1 Grid Element Container and Combinatorial Map Structure

As is indicated in Section 2.1 we use grids and multivalued maps to translate between the continuous nonlinear world we are interested in and the combinatorial world we may compute in. This suggests the need for a programmatic interface to construct and interact with grids. In our approach the grid elements themselves are identified with integers. The geometric objects of interest may be problem dependent and hence take the form of type `Geo`. Basic requirements are that the grid must provide methods for us to translate back and forth, as well as provide us access to a complete list of grid elements. Furthermore we need to be able to adaptively subdivide these grids. This leads to the following constructs.

1. `iterator`: A device used to loop through all grid elements in the grid \mathcal{X} .
2. `geometry`: A method for producing the `Geo` object associated with a grid element.

3. **cover**: A method for producing a set of grid elements which are known to provide an outer cover of a **Geo** object.
4. **subdivide**: A method to change the structure of the grid by subdividing a grid element into smaller pieces.
5. **complex**: A method to produce a cell complex out of a collection of grid elements.

For the computations presented in this paper we use a grid based on multiscale cubical structures and deal exclusively with **Geo** objects which are rectangular prisms. This can be generalized without breaking the above interface.

Our representation of the dynamics is based on multivalued maps which are outer approximations. Thus **cover** produces enough grid elements to form an outer cover of the geometric region provided.

To capture the dynamics of $F_\zeta: \mathbb{R}^n \times |\zeta|$ for a given $\zeta \in \mathcal{Z}$ requires a problem dependent computer routine \mathbb{F}_ζ that takes as input a **Geo** object A (think rectangular prism) and outputs a **Geo** object B , with the property that any point $F_\zeta(A, |\zeta|) \subset B$. With the routine \mathbb{F}_ζ the multivalued map can be obtain by simple composition

$$\mathcal{F}_\zeta = \text{cover} \circ \mathbb{F}_\zeta \circ \text{geometry}.$$

That is, we begin with a grid element, query the grid to recover a **Geo** object, apply the user-defined map function to produce another **Geo** object, and then cover this output with grid elements.

The grid provides a covering of the space in terms of topologically simple objects. However, to compute homology requires the finer structure of a cell complex. For simple grids consisting of cubes and simplices, the action of **complex** is classical. The use of more sophisticated grids requires the user to construct the appropriate **complex** operations.

3.2 Graph Theory Algorithms

For each $\zeta \in \mathcal{Z}$, the Morse graph MG_ζ is defined in terms of the multivalued map \mathcal{F}_ζ and provides a decomposition of the global dynamics. There are two essential computations associated with the construction of MG_ζ from \mathcal{F}_ζ : identification of the strongly connected path components and the partial

order between these components which we refer to as *reachability*. Both memory and run time are critical issues that need to be addressed.

We begin by remarking that the the computations are done in an adaptive manner; working with a uniform cubical grid decomposition of $X \subset \mathbb{R}^n$ is prohibitively expensive in both time and memory. A description of an adaptive procedure is presented in Ref. [2].

Tarjan's Algorithm is a standard procedure for computing strongly connected components.^[3] It proceeds by executing a depth first search and keeping track of so-called low-link information. Tarjan's algorithm requires time linear in the number of edges of the graph. It is important to note that storing \mathcal{F}_ζ can be memory intensive. The number of vertices is related to the size and dimension of $\text{Inv}(X, F_\zeta)$ and the number of edges associated with each vertex is determined by the product of the eigenvalues of Df with magnitude greater than one. An approach to circumventing this problem is to avoid storing \mathcal{F}_ζ and instead using \mathbb{F}_ζ , recompute $\mathcal{F}_\zeta(\xi)$ whenever necessary. Naively running Tarjan's algorithm with this approach leads to recomputing $\mathcal{F}_\zeta(\xi)$ many times for each grid element. Since these geometric computations can be quite expensive (especially in the context of differential equations), this is unacceptable. We remark that we have implemented a modified version of Tarjan's algorithm such that we do not store the entirety of \mathcal{F}_ζ in memory and yet only have to evaluate $\mathcal{F}_\zeta(\xi)$ once for each $\xi \in \mathcal{X}$.^[8] More precisely, there exists a strongly connected components algorithm which require $O(V)$ space, $O(E)$ time, and needs to query each vertex for its set of out-edges exactly once.

Turning to the issue of computing reachability, there are no known linear time algorithms. The reason for this is easy to see: consider concatenating two bipartite graphs so we obtain three layers. The reachability relation from the first layer to the third layer can be found by multiplying two matrices together. Conversely, a boolean matrix multiplication problem can be recast as a graph reachability problem in this fashion. Hence a reachability algorithm linear in the number of edges would correspond to an $O(n^2)$ boolean matrix multiplication algorithm for $n \times n$ matrices. The naive method of boolean matrix multiplication has complexity $O(n^3)$, however. While subcubic multiplication methods are indeed known, the best exponent on matrix multiplication doesn't correspond to a practical algorithm. However, it is conceivable that some very nice algorithm does exist, and there exists a corresponding reachability algorithm that can be executed in worst case $O(E \log E)$ time. This would require a major breakthrough, so we content ourselves with an

$O(EV)$ algorithm.

Since we are not interested in the entire reachability relation, but only the reachability relation between Morse sets, the problem becomes somewhat easier. Because current computers deal in 64-bit words, it is possible to establish the reachability relation for up to 64 Morse sets in a single pass of the edges (which we process in topological order). If there are more than 64, we require multiple sweeps. Since in practice we have a low number of Morse sets, we effectively find the reachability relation in linear time.

3.3 Conley Index Algorithms

There are two issues associated with the Conley index. First, we need to be able to compute the relative map on homology of an index pair. Second, we need to be able to identify shift equivalence classes on homology induced by the index maps.

There are two essential challenges to computing the relative homology of maps from the combinatorial data contained in \mathcal{F}_ζ . The first is to identify chain maps which carry the appropriate information. Our approach is to consider the graph Γ of the multivalued map \mathcal{F}_ζ . Under reasonably weak conditions the homology of Γ is isomorphic to the homology of the domain and the projection maps π_d and π_r from Γ to the domain and range, respectively, are chain maps.^[9, 19] Thus, in this setting

$$\mathcal{F}_{\zeta*} := \pi_{r*} \circ \pi_{d*}^{-1}$$

provides an appropriate map on homology.

The second challenge arises from the fact that the cell complex representing Γ can be quite large. Because of this, we have developed an algorithm that can compute the induced map of homology of a relative map $\mathcal{F}: (X, A) \rightarrow (Y, B)$ which finds cycles in the domain (X, A) and proceeds to lift them into a corresponding cycle in (Γ_X, Γ_A) . This procedure only needs to construct a single graph fiber at a time, and thus can have significantly lower memory requirements.^[9]

The computation of shift equivalence classes appears to be an open problem except in special cases. Fortunately one such special case is that of vector spaces over finite fields. In this case it is possible to identify shift equivalence class of a matrix A by computing the Smith Normal Form of the matrix $A - Ix$. From this one acquires invariant factors and factors the

largest power of x possible; if one is left with 1 the factor is discarded. What remains characterizes the shift equivalence class.

3.4 Continuation Algorithms

As is indicated in Section 2.4 the concepts of continuation are based on the existence of clutching graphs. Computationally, we are presented with two Morse decompositions $\{\mathcal{M}_\zeta(p) \subset \mathcal{X} \mid p \in \mathcal{P}_\zeta\}$ and $\{\mathcal{M}_{\zeta'}(p') \subset \mathcal{X} \mid p' \in \mathcal{P}_{\zeta'}\}$. Let n be the number of grid elements in all the Morse sets of both Morse decompositions. The following naive algorithm computes the clutching graph in $O(n^2)$ time. Use an outer loop which loops through every grid element in a Morse set in the first grid, and an inner loop that loops through the grid elements of the Morse sets of the second grid. Whenever an intersection is found, an edge in the clutching graph is forged. This naive algorithm, though generally applicable, is woefully inefficient. In practice, we re-express the Morse sets in one grid by covering them in the other. After this step, what remains is to scan grid elements, which takes linear time. Thus the complexity bottleneck is determined by how hard it is to cover a set of grid elements from $\cup_{p \in \mathcal{P}_\zeta} \mathcal{M}_\zeta(p)$ with grid elements from $\cup_{p' \in \mathcal{P}_{\zeta'}} \mathcal{M}_{\zeta'}(p')$, and vice versa. This, in turn, depends on the details of the grid implementation. For hierarchical tree-based multiscale cubical structures where the outer bounds of the grid are the same, we obtain an $O(n)$ algorithm.

Having determined the clutching graphs it is easy to identify the Morse continuation classes and Morse Graph continuation classes via generating relations. However, we require a data structure which takes these generating equivalences as input and provide us with a representation of the equivalence classes. This is a classical problem and hence we employ the *disjoint set data structure*, also known as a *union-find* structure. This structure, when initialized, regards some finite set of elements as each belonging to disjoint singleton sets. By calling a `union` method, these sets may be unioned together until the disjoint set data structure represents the partition associated with the equivalence relation. (The `find` method is used to determine a representative element of each disjoint set; so it can be used to determine if two elements are equivalent). The `union` and `find` methods are not constant time, but rather the time complexity is given by the inverse Ackermann function.^[21] For all practical purposes we may consider inverse Ackermann to be constant time, as it grows *extremely* slowly. Given the union-find structure, what remains to us is simply to produce a generating set of relations to learn the equivalence

classes. For each generating equivalence, we call the `union` method.

3.5 Database Structure

The desired result of our computations is a database from which one can extract useful information concerning the dynamics. This information takes the form of a collection of *records*:

1. **Parameter Record:** Indicate a region of parameter space and give it an index so it may be cross-referenced by other records.
2. **Morse Record:** Indicate the Morse graph associated to some parameter record.
3. **Continuation Record:** Indicate the clutching graph associated to some indicated pair of parameter records.
4. **Conley Record:** Indicate the Conley index associated with some indicated Morse set associated to some indicated Morse Record.

If we only have records of type (1)-(3), we call it a *Morse Graph database*. If, on the other hand, we have all types of records, it is a *Conley-Morse Graph database*. In our computations, we first produce a Morse Graph database, and then process the continuation records using a union-find structure in order to learn the Morse continuation classes. Then we choose a single representative of that class, and compute the “Conley Record” associated with it. By Corollary 2.16 the Conley index is constant on continuation classes of Morse sets. Clearly, this is much more efficient than performing expensive Conley Index computations to produce Conley Records for every Morse set of every Morse Record.

3.6 Query Algorithms

Once we obtain the database structure, we make use of it via *database queries*. Because the records make reference of each other, it is possible to make a number of different queries. Examples include, but are not limited to:

1. Identify all parameter regions in the same Morse Graph continuation class.

2. Identify all Morse Graph continuation classes for which we have shown multiple basins of attraction exist.
3. Identify all Morse Graph continuation classes which contain a Morse set with a given Conley Index.

4 Applications

In order to demonstrate the potential of our approach, we present two applications of the computational framework introduced in the previous sections.

4.1 Three Age-Classes Overcompensatory Leslie Model

Consider the following three-age class overcompensatory Leslie population model.

$$\begin{cases} x = (\theta_1 x + \theta_2 y + \theta_3 z)e^{-0.1(x+y+z)} \\ y = 0.7x \\ z = 0.7y \end{cases} \quad (6)$$

The variables x , y , and z represent the age class populations in order of ascending age. If one views this as a model of a plant population, then the parameters 3 parameters $\theta_i, i = 1, 2, 3$ can be interpreted as the seed production rates of the different age classes. The exponential term represents an overcrowding factor that depends on the adult population. This model and its biological relevancy is discussed in greater detail in Ref. [22].

To set up the computations we choose the parameter region of interest:

$$Z := \{(\theta_1, \theta_2, \theta_3) \mid 14.5 \leq \theta_1 \leq 30.5, 13.0 \leq \theta_2 \leq 37.0, 13.0 \leq \theta_3 \leq 37\} \subset \mathbb{R}^3.$$

The parameter space grid \mathcal{Z} is constructed by subdividing Z into 32 equal sized intervals in each direction. This divides parameter space into 32768 three dimensional cubical cells. To speed up the computation, we choose to compute for sets of parameter values that are represented by the edges in this complex. Thus, there are a total of 104544 one dimensional parameter boxes for which we produce a Conley Morse graph.

The compact region in phase space is given by

$$X := [0, 320.056] \times [0, 224.040] \times [0, 224.040] \subset [0, \infty)^3.$$

It can be shown analytically that X is an isolating neighborhood for the global attractor of (6) for all $\theta \in Z$. Using an adaptive subdivision algorithm similar to that of Ref. [2] the final grid in phase space consists of cubes obtained by subdividing X into 2^{12} equal sized intervals in each direction. In general this produces Morse decompositions consisting of many Morse sets most of which are spurious in the sense that the recurrence is due to numerical error. To eliminate obvious spurious solutions the cubes in each Morse set are once again subdivided up to 2^4 times in each direction and recurrence within this regions is checked. If the recurrence disappears then one can safely conclude that the associated region in phase space does not contain recurrent dynamics. For a more detailed discussion of this step see Ref. [2].

The computation based on the above mentioned inputs was run on 15 nodes of a cluster, using 3 processors per node. Each node had a minimum of 8 GB of memory. The total computation time was 137 hours, of which 134 hours were needed to find the Morse graphs.

As is indicated in the Introduction an important impetus behind the database is to be able to quickly and efficiently find interesting dynamics. Given that this is a population model a natural question has to do with the structure of attractors and/or the existence of multiple attractors as a function of the parameter values.

Let us begin by considering the existence of multiple attractors. The appropriate query is to ask for those nodes in the continuation graph for which the associated Morse graphs contain more than one minimal node. To make the results visibly manageable we restrict our attention to the larger continuation classes. In particular, Figure 2 shows the continuation graph for the 15 largest continuation classes. These 15 continuation classes are associated with 103593 of the 104544 grid elements of parameter space which implies that over 99% of parameter space is accounted for. The boxed nodes represent Morse graphs with multiple minimal nodes and therefore for the corresponding parameter values there are multiple basins of attraction. Observe that there are three mutually adjacent continuation classes with multiple attractors. The sizes of these parameter regions are 13964, 5222, and 1497 parameter boxes. Thus in roughly 20 percent of the parameter space we study we can guarantee the existence of at least two basins of attraction.

We now turn to the question of identifying the structure of the dynamics in the attractors. In particular we make use of the following language.

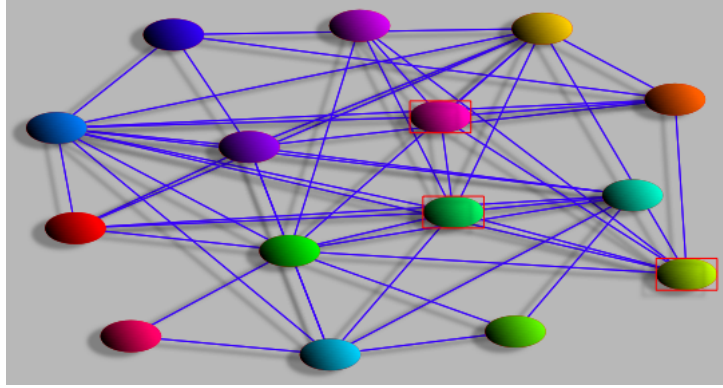


Figure 2: Continuation Graph showing the 15 largest continuation classes for the system (6). The boxed nodes represent Morse graphs with multiple minimal nodes which implies that at the corresponding parameter values there exist multiple basins of attraction. The yellow class contains 13964 boxes, the pink class contains 5222 boxes, and the green class contains 1497 boxes.

Definition 4.1. An isolated invariant set S for a map $f: X \mapsto X$ is a T -cycle set if there exist T disjoint, compact regions N_1, \dots, N_T such that $S = \text{Inv}(N, f)$ where $N := \cup_{i=1}^T N_i$ is an isolating neighborhood, and

$$f(N_i \cap N) \subset N_{i+1}, i = 0, \dots, T - 1$$

where $N_0 := N_T$.

Consider the the continuation class with 13964 nodes. The associate Conley Morse graph as shown in Figure 3. Recall that the bracketed numbers identify the Morse set continuation class (MSCC) of each node in the graph. The Conley Index of MSCC [0] is trivial except in dimension zero, where it has invariant factor $x + 1 \pmod 2$. By Proposition 5.8 in Ref. [2] we conclude that the associate Morse set is a 1-cycle set. More specifically there is an associated isolating neighborhood which is contractible and maps strictly to its interior under the dynamics of (6).

As is indicated in Section 2.4 the above mentioned description in terms of the 1-cycle set extend to the entire Morse set continuation class MSCC[0]. The three boxed nodes in Figure 4 indicate Morse set continuation classes over which MSCC[0] extends.

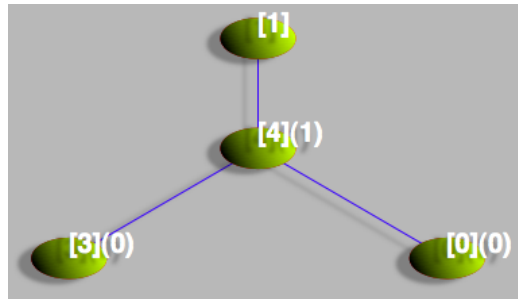


Figure 3: Conley Morse graph for the continuation class with 13964 nodes in Figure 2.

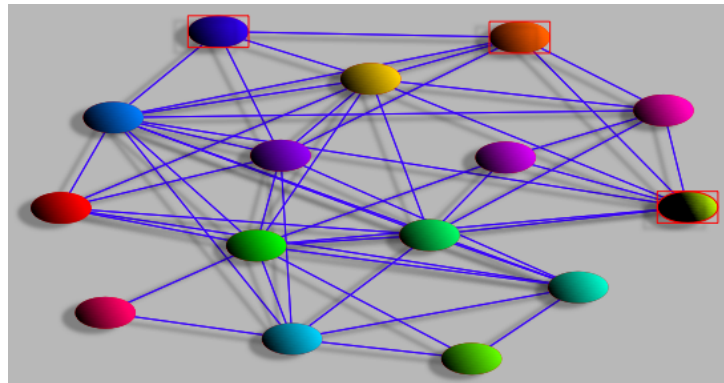


Figure 4: Boxed nodes representing the continuation classes over which the Morse set continuation class of MSCC[0] in Figure 3 extends to.

The other attractor, MSCC[3], has Conley Index which is trivial except in dimension zero where it is represented by the invariant factor $x^4 + 1 \pmod 2$. This is characteristic of a 4-cycle set. The extent of this Morse set continuation class is given by the boxed nodes in the continuation graph in Figure 5.

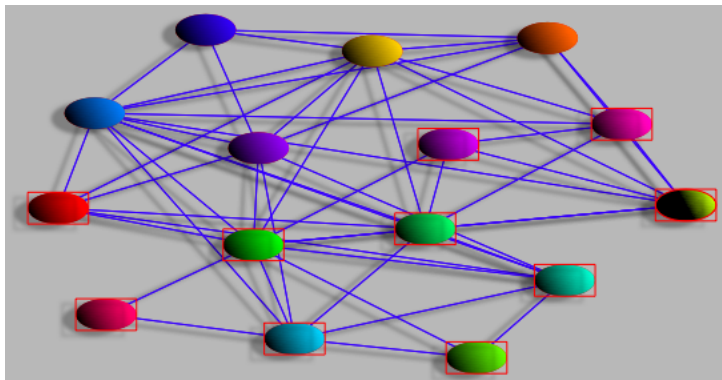


Figure 5: Boxed nodes representing the continuation classes over which the Morse set continuation class of MSCC[3] in Figure 3 extends to.

Observe that the nodes in the continuation graph which are not boxed in either Figure 4 or Figure 5 must contain another distinct attracting Morse set continuation class. It appears, for example, as MSCC5 in the Morse graph shown in Figure 6. The Conley Index of MSCC[5] in dimension zero is represented by $x^2 + 1$, which is characteristic of a 2-cycle set. Among the fifteen largest continuation classes, these are all of the Morse set continuation classes of attractors that appear.

Observe that we have characterized the attractors for a large fraction of parameter space. However, because of the concern of extinction in the context of small perturbations biologists often are interested in understanding when the attractor is bounded away from the states of extinction. This is often called persistence or permanence (see Ref. [10] for a precise definition and further discussion). In the setting of this model extinction can be identified with the origin. We remark that the origin appears in the database as MSCC[1]. It can also be checked that MSCC[1] extends over all of the fifteen largest continuation classes (see Figure 7). Furthermore, in none of these cases is it an attracting Morse set (special cases of this can be seen in Figures 3 and 6). Since the computations have been done at a minimal fixed scale we can conclude that (6) exhibits persistence.

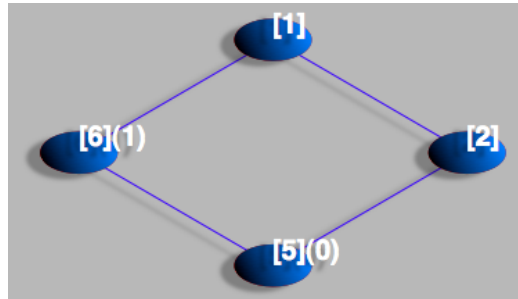


Figure 6: A Morse graph with an attractor that belongs to the Morse set continuation class $\text{MSCC}[5]$.

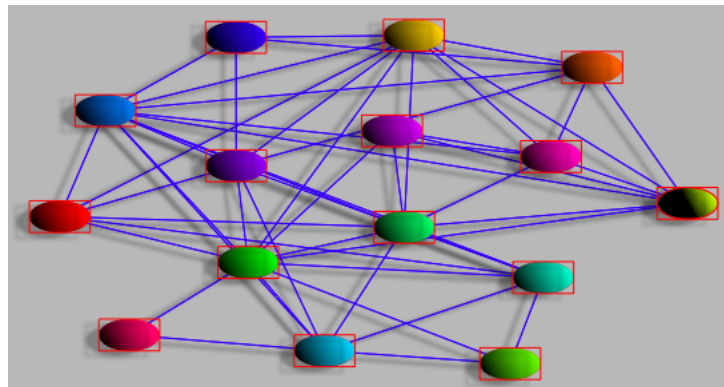


Figure 7: Boxed nodes indicate continuation classes for which the Morse set containing the origin is not an attractor.

Of course there are additional questions that can be asked concerning the dynamics of (6). For some of these additional database queries can prove useful. However, we hope that in the context of attractors, which is the most reasonable entry point for questions concerning biologically observable phenomena, we have made it clear that the database provides sufficient information to obtain useful nontrivial answers.

4.2 Three-dimensional coupled map lattice

Another example application of Conley-Morse Database software is the Coupled Map Lattice (CML), a coupled system of maps introduced by K. Kaneko and others independently around early 1980's, see Ref. [13] and references therein for more information.

The n -CML is an n -dimensional dynamical system $F: \mathbb{R}^n \rightarrow \mathbb{R}^n$, with $F(x) = (F_1(x), \dots, F_n(x))$ for $x = (x_1, \dots, x_n)$ given by

$$F_i(x) = (1 - \varepsilon)f_a(x_i) + \frac{1}{2}(\varepsilon - \delta)f_a(x_{i-1}) + \frac{1}{2}(\varepsilon + \delta)f_a(x_{i+1})$$

$$i = 1, \dots, n,$$

where $x_0 = x_n$ and $x_{n+1} = x_1$. This system has three parameters, a , ε , and δ . In this paper, we choose f_a to be the logistic map, $f_a(\xi) = 1 - a\xi^2$.

There is a well-studied similar coupled dynamical system known as the Globally Coupled Maps (GCM)^[14] defined by

$$F(x)_i = (1 - \varepsilon)f_a(x_i) + \frac{\varepsilon}{n} \sum_{j=1}^n f_a(x_j) \quad i = 1, \dots, n.$$

As an important feature of CML, as compared to GCM, CML is a non-symmetric coupling, and as a result, CML exhibits a traveling wave at some parameters. In order to study the traveling waves more closely, M. Komuro (personal communication) examined the 3-CML in detail, using conventional numerical analysis. The object corresponding to traveling waves in 3-CML is an invariant closed circle (ICC), which can be observed numerically in a region of the (a, ε) -parameter plane of 3-CML with fixed $\delta = 0.06$. See Figures 8 and 9 for a numerically generated bifurcation diagram obtained by M. Komuro using the numerical method proposed in Ref. [15].

Below, we describe the result of computation of the 3-CML using the Conley-Morse Database software. In fact, the actual computation was done

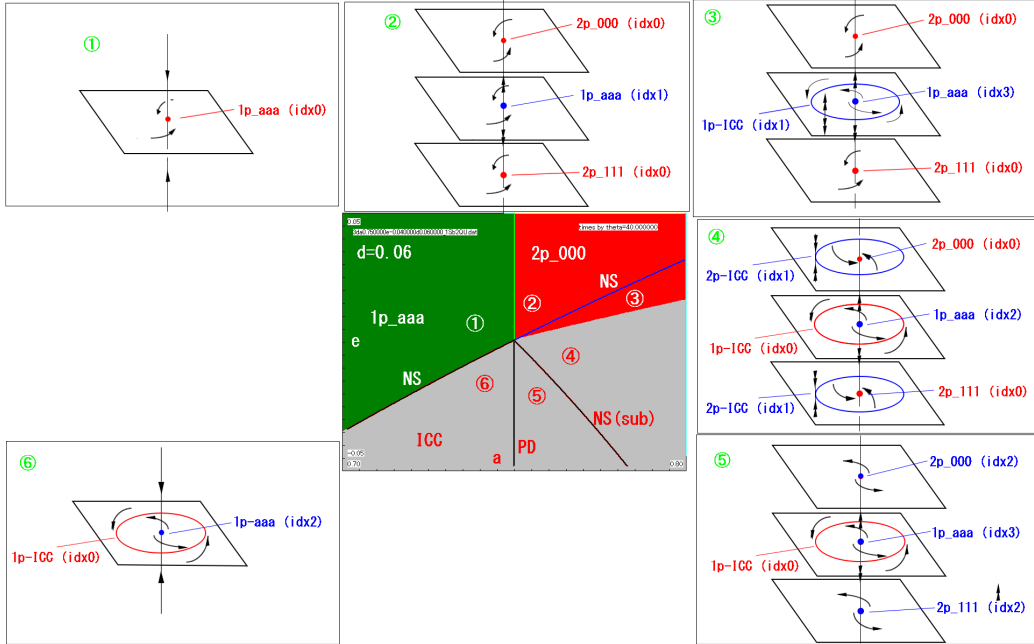


Figure 8: The numerically generated bifurcation diagram (colored plate in the center) and corresponding schematic phase portraits for 3-CML, obtained by M. Komuro. The parameter range is chosen to be $[0.7, 0.8] \times [-0.05, 0.05]$ with $\delta = 0.06$, which is divided into six regions, numbered by circled numerals. Each parameter region corresponds to the plate numbered by the same circled numeral. The ICCs appear in Regions 3–6. Especially, in Region 4, there exist multiple ICCs, the unstable one being periodic with period two under the action of 3-CML. Figure courtesy of M. Komuro.

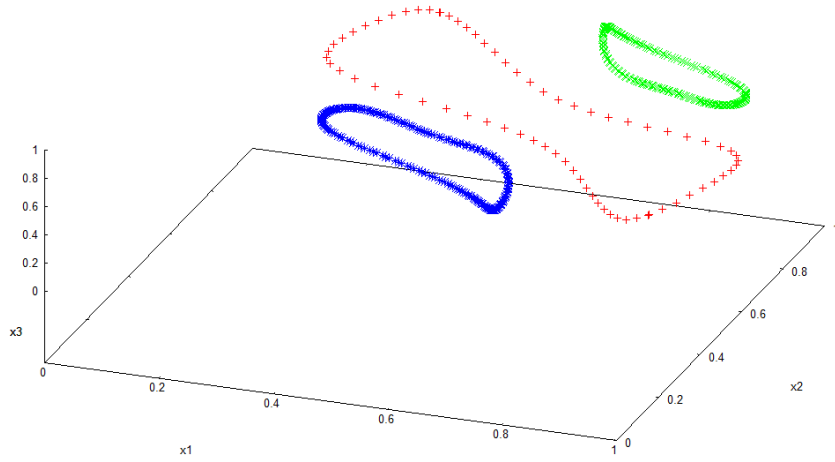


Figure 9: The invariant circles appearing in Region 4 in Figure 8, computed numerically by M. Komuro. Figure courtesy of M. Komuro.

using the first version of the software explained in Ref. [2], as the latest version of the software discussed in the previous sections was not yet fully available at the time of the computation.

The computation parameters are taken as follows:

- (a, ε) varies in $[0.72, 0.79] \times [-0.02, 0.04]$
- δ is fixed to 0.06.

Note that in this parameter region, f_a has attracting period-2 periodic points. The box of $[0.72, 0.79] \times [-0.02, 0.04]$ is divided into 16×16 small boxes, and we take the center of each box as the input parameter value for each computation. As the interval arithmetic is used in the software, we could have taken the entire small boxes as the input parameters for the computations, but this would have been much more time consuming, and the overestimates would require us to use a finer grid in the parameter space. The phase space for the logistic map is taken as $[-1.1, 1.1]$, hence the entire phase space is $[-1.1, 1.1]^3$, on which we put the uniform grid decomposition into $2^9 \times 2^9 \times 2^9$ boxes. When needed, we set the refinement level of subdivision as 4, in case the computation result is not sufficient.

The Conley-Morse graph and corresponding phase space structure for each parameter region in Figure 10 is shown in Figure 11. These results agree well with the bifurcation structure shown in Figure 8.

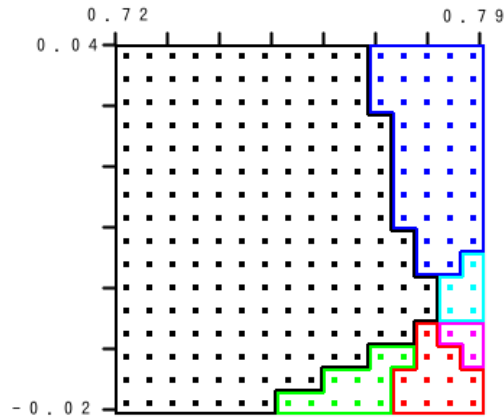


Figure 10: The bifurcation diagram computed by the Conley-Morse database software. Compared to Figure 8, the number of divided regions of the parameter domain agrees, but each region is a little tweaked, which is mainly due to the overestimation by the construction of multivalued maps.

5 Acknowledgments

M.G. acknowledges the support of Fapesp Processo 2010/00875-9 and CNPq Processo 306453/2009-6. H.K. acknowledges the support of Ministry of Education, Science, Technology, Culture and Sports, Japan, Grant-in-Aid for Scientific Research No. 21340035. The work of K.M., S.H., and J.B. was partially supported by NSF grants DMS-0915019 and CBI-0835621 and by contracts from DARPA and AFOSR. P.P. acknowledges the support from the E.U. and Portuguese national funds received through Fundação para a Ciência e a Tecnologia (FCT), project FCOMP-01-0124-FEDER-010645 (ref. FCT PTDC/MAT/098871/2008) and Est-C/MAT/UI0013/2011.

References

- [1] Z. Arai, M. Gameiro, T. Gedeon, H. Kokubu, K. Mischaikow, and H. Oka, “Graph-based topological approximation of saddle-node bifurcation in maps,” RIMS Kokyuroku Bessatsu, to appear.

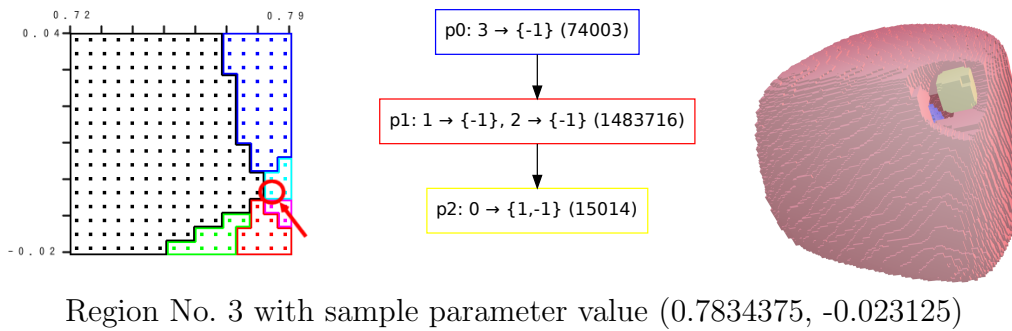
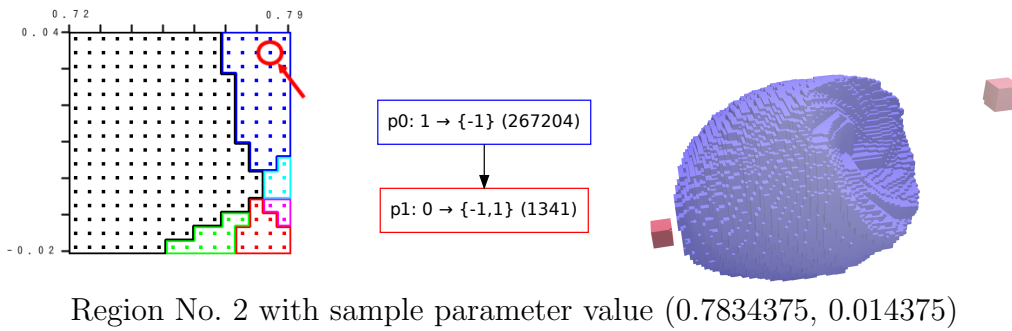
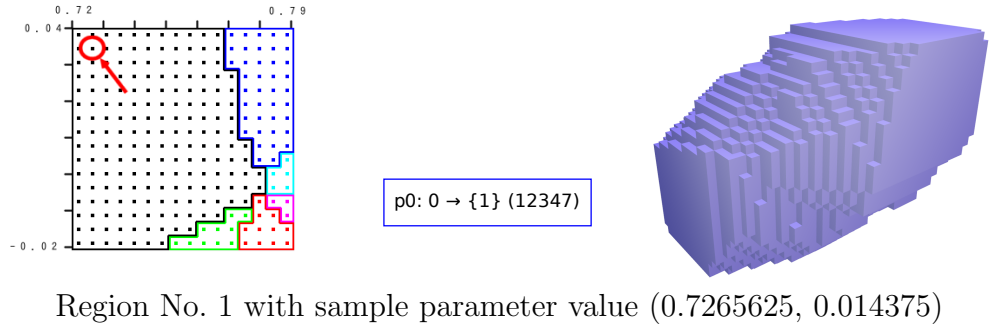
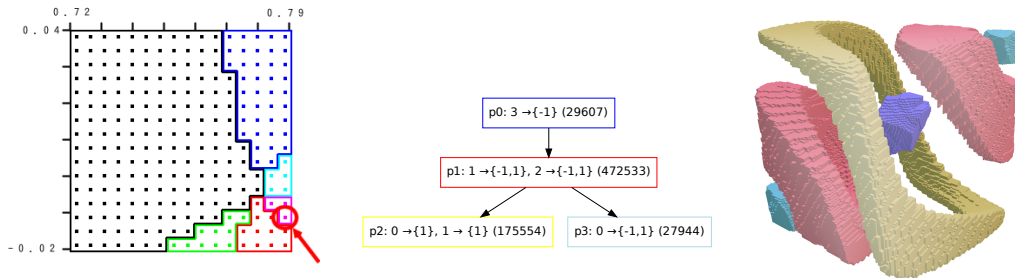
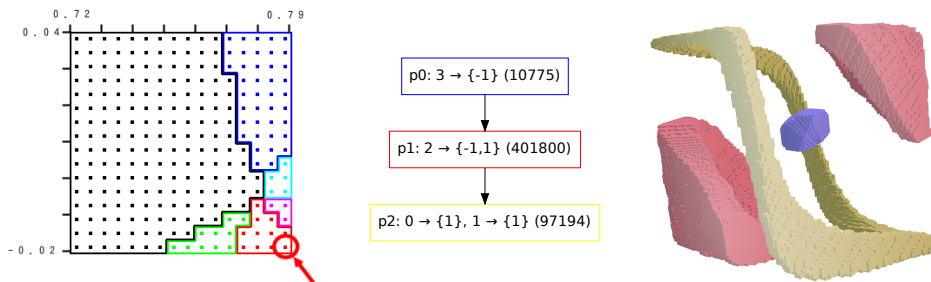


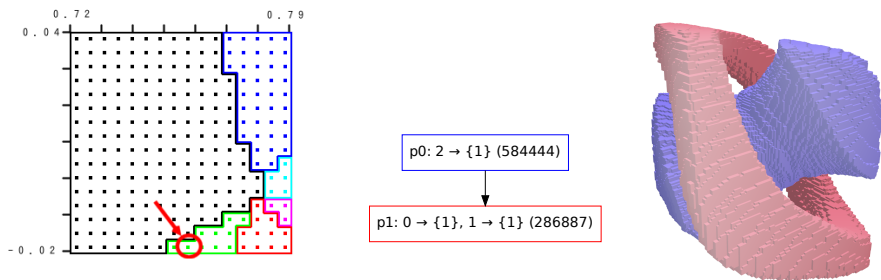
Figure 11: Results of the computations for the 3-CML. For each Morse graph continuation class, a Conley-Morse graph and the corresponding Morse sets are plotted for a sample parameter point. The choice of the parameter for each class is marked with a red circle at the left-hand side, the Conley-Morse graph for the parameter is drawn in the center, and the Morse sets for the parameter appear at the right-hand side.



Region No. 4 with sample parameter value (0.7878125, -0.030625)



Region No. 5 with sample parameter value (0.7878125, -0.038125)



Region No. 6 with sample parameter value (0.7571875, -0.038125)

Figure 11: (Continued)

- [2] Z. Arai, W. Kalies, H. Kokubu, K. Mischaikow, H. Oka, and P. Pilarczyk, “A database schema for the analysis of global dynamics of multi-parameter systems,” *SIAM J. Appl. Dyn. Syst.* **8**, 757–789 (2009).
- [3] T. Cormen, C. Leiserson and R. Rivest, *Introduction to algorithms*, The MIT Electrical Engineering and Computer Science Series, (MIT Press, Cambridge, MA, 1990).
- [4] S. Day, O. Junge, and K. Mischaikow, “A rigorous numerical method for the global analysis of infinite-dimensional discrete dynamical systems,” *SIAM J. Appl. Dyn. Syst.* **3**, 117–160 (2004).
- [5] S. Day, Y. Hiraoka, K. Mischaikow, and T. Ogawa, “Rigorous numerics for global dynamics: A study of the Swift-Hohenberg equation,” *SIAM J. Appl. Dyn. Syst.* **4**, 1–31 (2005).
- [6] J. Franks and D. Richeson, “Shift equivalence and the Conley index,” *Trans. Amer. Math. Soc.* **352**, 3305–3322 (2000).
- [7] M. Gameiro, T. Gedeon, W. D. Kalies, H. Kokubu, K. Mischaikow, and H. Oka, “Topological horseshoes of traveling waves for a fast-slow predator-prey system,” *Journal of Dynamics and Differential Equations* **19**, 623–654 (2007).
- [8] S. Harker and K. Mischaikow, ”Topological sort for graphs with large numbers of edges,” in preparation.
- [9] S. Harker, K. Mischaikow, M. Mrozek, and V. Nanda, “Discrete Morse theoretic algorithms for computing homology of complexes and maps,” in preparation.
- [10] V. Hutson and K. Schmitt, “Permanence and the dynamics of biological systems,” *Mathematical Biosciences*, **111** 1–71 (1992).
- [11] T. Kaczynski, K. Mischaikow, and M. Mrozek, *Computational homology*, Applied Mathematical Sciences, vol. 157 (Springer-Verlag, New York, 2004).
- [12] W. D. Kalies, K. Mischaikow, and R. C. A. M. Vandervorst, “An algorithmic approach to chain recurrence,” *Found. Comput. Math.* **5**, 409–449 (2005).

- [13] K. Kaneko, “Overview of coupled map lattices,” *Chaos* **2**, 279–282 (1992).
- [14] K. Kaneko, “Clustering, coding, switching, hierarchical ordering, and control in a network of chaotic elements,” *Physica D* **41**, 137–172 (1990).
- [15] K. Kamiyama, M. Komuro, and T. Endo, “Bifurcation of quasi-periodic oscillations in mutually coupled hard-type oscillators —Demonstration of unstable quasi-periodic orbits—,” *International Journal of Bifurcation and Chaos*, to appear.
- [16] K. Mischaikow, M. Mrozek, J. Reiss, and A. Szymczak, “Construction of symbolic dynamics from experimental time series,” *Phys. Rev. Lett.* **82**, 1144–1147 (1999).
- [17] K. Mischaikow and M. Mrozek, “Conley index,” in *Handbook of Dynamical Systems*, vol. 2, pp. 393–460 (North-Holland, Amsterdam, 2002).
- [18] K. Mischaikow and M. Mrozek, “Chaos in the Lorenz equations: A computer-assisted proof,” *Bull. Amer. Math. Soc.* **32**, 66–72 (1995).
- [19] K. Mischaikow, M. Mrozek, and P. Pilarczyk, “Graph approach to the computation of the homology of continuous maps,” *Found. Comput. Math.* **5**, 199–229 (2005).
- [20] M. Mrozek, “An algorithm approach to the Conley index theory,” *J. Dynam. Differential Equations* **11**, 711–734 (1999).
- [21] R. E. Tarjan and J. van Leeuwen. ”Worst-case analysis of set union algorithms,” *Journal of the ACM*, **31**(2), 245–281 (1984).
- [22] I. Ugarcovici and H. Weiss, “Chaotic dynamics of a nonlinear density dependent population model,” *Nonlinearity* **17** 1689–1711 (2004).